

Accurate Signal Recovery in UHF Band Reuse-1 Cellular OFDMA Downlinks

Giridhar K ¹ and Abhay Mohan M V ²

¹Affiliation not available

²Indian Institute of Technology Madras

October 30, 2023

Accurate Signal Recovery in UHF Band Reuse-1 Cellular OFDMA Downlinks

Abhay Mohan M. V. and K. Giridhar

Abstract

Accurate signal recovery is challenging for non-co-located transmit antennae deployments due to Inter Tower Interference (ITI) in reuse-1 cellular OFDMA networks. In the sub-1 GHz UHF band where only SISO deployment is possible, interference aware receiver algorithms are essential to mitigate the ITI. In this work, we develop a Joint Modified Least Squares (JmLS) algorithm for channel estimation in the presence of ITI. Firstly, it is shown that the JmLS algorithm achieves the Cramer-Rao lower bound. Next, an approach to managing the possibly distinct carrier frequency offsets of the different co-channel signals of interest is proposed. This improves the quality of the bit-level Joint Log-Likelihood Ratio. Finally, the impact of the choice of pilot sub-carrier information in the block modulated air-interface on the coded block error rate performance is studied. In particular, a comparison is made between (i) frequency orthogonal pilots from the different sectors, vis-a-vis, (ii) a pilot-on-pilot arrangement using pseudo-orthogonal sequences. The study indicates that based on the extent of frequency selectivity and the number of interferers being considered, (ii) is advantageous when the set of ITI pilots incident on a receiver is small when compared to the set of all possible pilots.

Index Terms

Carrier Frequency Offset compensation, Co-channel interference, Intercarrier Interference, Inter-tower Interference, Joint Channel Estimation, Joint Detection, Joint LLR, Least Squares Channel Estimation, OFDMA, UHF Cellular systems.

Abhay Mohan and K. Giridhar are with the Department of Electrical Engineering, Indian Institute of Technology Madras, Chennai 600 036, India (e-mail: abhay@tenet.res.in; giri@tenet.res.in).

I. INTRODUCTION

Current 4G-LTE or the emerging 5G-NR wireless standards based broadband cellular networks use universal frequency reuse. In such OFDM/OFDMA block-modulated networks, universal frequency reuse or reuse-1 is used network wide, where the same frequency resource is used by all cell towers and sectors¹ in order to provide a higher sum throughput. This increased throughput is possible by employing one or more techniques (see for example [1], [2]) to manage the increased inter tower interference (ITI) caused by such a reuse-1 deployment. Cellular OFDMA networks deployed in the Ultra High Frequency (UHF) bands can provide excellent geographical coverage. However, since only Single Input Single Output (SISO) links are possible in the UHF band due to the large wavelengths, spatial filtering is not possible and the ITI has to be removed purely by better signal processing algorithms.

While some amount of ITI avoidance in cellular OFDM networks is possible by using fractional frequency reuse or soft frequency reuse [3]–[5], ITI mitigation by carefully estimating its impact on different parameters in the measurement model is the focus of this work. In particular, in downlink ITI models, the different modulated signals will not only travel through different channel responses, but also carry different carrier frequency offsets (CFOs) and time-of-flight values. Each CFO term could in turn be seen as a sum of the the voltage controlled oscillator (VCO) induced error and the Doppler induced error. The extent of contribution of each of these errors on the total CFO error can vary on a case to case basis. In the current work, an implicit assumption is made that the CFO error present in each of the ITI signals is primarily contributed by the oscillator frequency mismatch (see footnote in page 6) between that transmitter and the user equipment (UE).

In OFDM systems, there is generally a tight specification on the maximum CFO error. This is important because as shown in [6], in order to have the signal power at least 20 dB greater than the total inter-carrier interference (ICI), the carrier frequency offset needs to be limited to less than 4% of the inter-carrier spacing. A work related to the current study is found in [7], which describes an uplink scenario involving coordinated joint detection of K users by M tower equipment. This is different from our downlink model where the UE only needs to decode the message from one of the towers

¹The word sector is used to refer to one part of the 360° region served by a cell site, or to simply one part of that region (typically a 120° portion, when 3 sectors are deployed per cell site). Here, the term inter-tower interference (ITI) subsumes the inter-sector interference that could be present at the sector boundaries.

while keeping in mind the interference structure caused by the other ITI terms. Nevertheless, the work in [7] also treats the problem of CFO in an OFDM based framework and hence has some similarity to our model.

The key contributions of our work are described below with reference to the block diagram in Fig. 1.

- 1) The modified Least Squares (mLS) technique in [8] is extended to a joint channel estimation setting where the desired as well as the ITI channels are estimated. This estimator is shown in the block labelled (A) in Fig. 1. These estimates are nearly interference-free even when the ITI pilots have equal or higher power than the desired pilots. The proposed framework is more tolerant to CFOs carried by the ITI signals by utilizing a particular time-domain de-rotation scheme applied on the received signal, labelled as (B) in the block diagram. Prior published work on joint channel estimation such as [9] and [10] have not explicitly addressed this problem. We call this approach the *Joint modified Least Squares* estimator. It is then shown to be an unbiased estimator that achieves the Cramer-Rao Lower Bound, and is hence the *minimum variance unbiased estimator* [11] (MVUE) for this problem. For the same power per subcarrier, JmLS outperforms orthogonal pilot based estimation by $10 \log_{10} M$ dB because it will have M times more pilots available as compared to an orthogonal pilot allocation over M adjacent towers.
- 2) The second novel contribution is the extension of the Joint Log Likelihood Ratio (JLLR) based detection framework discussed in [12] and [13] to work in the presence of distinct CFOs. JmLS estimates generated from mean-derotated received signal is fed into the JLLR along with a compensation factor (C) for the incremental phase ramp caused due to the frequency offset in the LLR expression. This detector will be referred to as the Offset Corrected Joint LLR (OC-JLLR) detector. Since the LLR is calculated considering the ITI structure, this joint detector manages both interference and CFO errors in an elegant way using only a single receive antenna. The Max-Log-MAP approximation [14] is used in the calculation of LLRs to reduce OC-JLLR complexity.

It should be noted that both of the proposed approaches for channel estimation and signal detection complement each other, because the JmLS channel estimates carry information on the amplitude and phase distortion caused due to CFOs to the Joint LLR detector. The OC-JLLR has a mechanism incorporated to track the incremental phase caused due to the residual CFO error.

This paper is organised as follows. In Section II, the system description is provided, which includes the assumptions made in deriving the measurement model. This will be followed by the description of the CFO modelling adopted in this paper in Section III. The Joint Channel Estimation is discussed in Section IV and the Joint Detection framework in Section V. The simulation results are presented in Section VI, and the work is concluded in Section VII.

A. Basic Notation

Bold symbols denote vectors or matrices. Capital letters usually denote frequency domain and small letters for time domain. Augmented vectors or block diagonal matrices will be underlined and a hat on top a parameter (e.g., \hat{x}) will represent an estimate of the parameter x . An N subcarrier OFDM system with M transmitters are considered. The transmitters are numbered from $0, 1, \dots, M - 1$, and the 0^{th} transmitter denotes the one that the UE is communicating to. The subscripts k and m are used to denote the k^{th} subcarrier and m^{th} tower. Finally, N_{block} denotes the turbo block length and Δf_{max} denotes the maximum carrier frequency offset.

II. SYSTEM DESCRIPTION

The downlink scenario of a multi-cell reuse-1 system where the UE receives co-channel signals from $M = 4$ towers is described in the block diagram shown in Fig. 1. All the towers transmit in the same subcarriers and typically carry different CFOs relative to the UE. These CFOs are denoted by $\Delta f_0, \Delta f_1, \dots, \Delta f_{M-1}$ and the CFOs normalized by the subcarrier bandwidth to yield $\epsilon_0, \epsilon_1, \dots, \epsilon_{M-1}$. The CFOs manifest as a phase rotation and amplitude scaling on the received symbol constellation after downconversion and conversion to frequency domain in the UE [15]. The OFDM symbols from each tower is rotated by different amounts due to the difference in CFOs and the received symbol will be a sum of all these faded, rotated OFDM symbols along with the measurement noise. The advanced receiver shown in the block diagram first applies a time domain compensation to the distortion caused by CFOs. It then performs joint estimation of the signal and interference channels followed by detection of the desired signal by modelling the interferers. The CFOs and the derotation factor derived to compensate for the CFOs are also input to the detector. These blocks shall be explained in detail in sections III, IV and V.

The assumptions made in this work are given below.

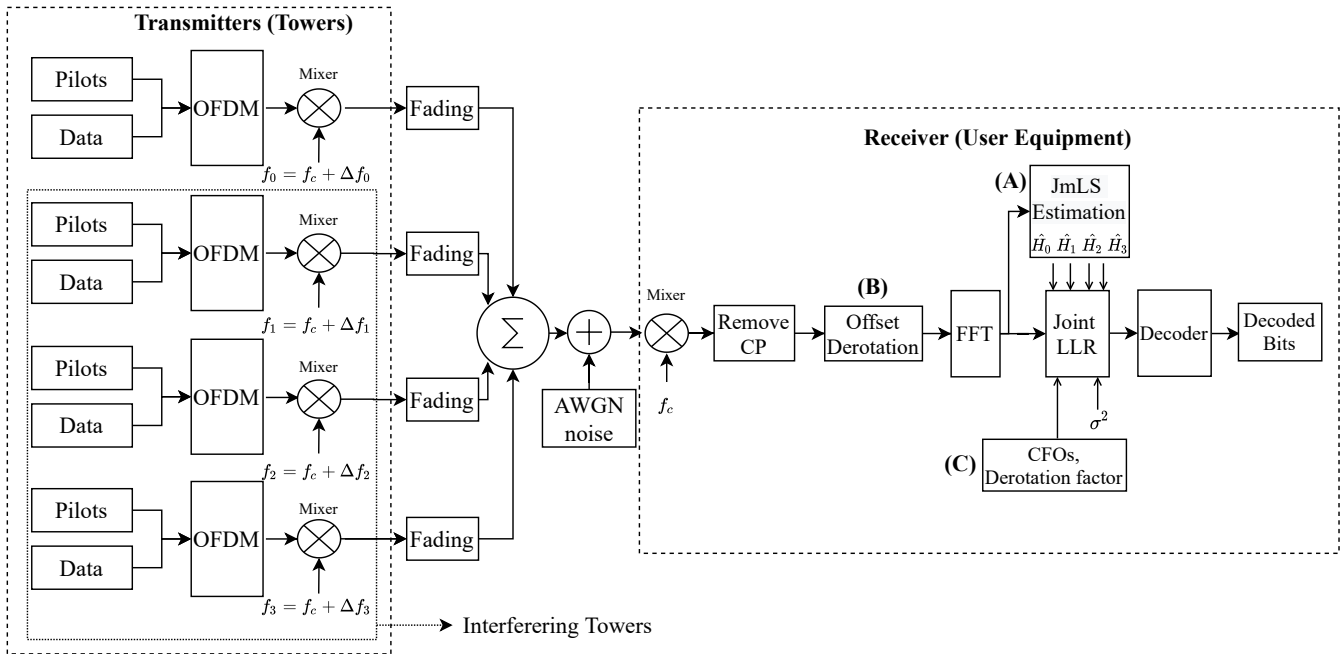


Fig. 1: Block diagram describing a system with three ITI signals and the proposed receiver structure.

- 1) The number of significant ITI signals and their corresponding CFOs and timing information are assumed to be known or accurately estimatable².
- 2) The signal modulation carried on each ITI stream is assumed to be known. In this work, we restrict our attention to only 4-QAM and 16-QAM constellations for simplicity. When this information is not known, modulation order classification techniques such as those described in [17] and [18] could possibly be used.
- 3) As mentioned in [8], it is assumed that an estimate of the maximum multipath delay spread T_m in samples among all the channels is known ($L = F_s T_m$). If this is not available, L is set to N_{cp} , the cyclic prefix length.
- 4) Knowledge of noise variance, σ^2 , is required. This can be estimated by measuring the average power of the received guard subcarriers.
- 5) The VCO induced frequency error is assumed to be the primary contribution to the CFO. Typically

²One way to accomplish this is using a two symbol preamble. Each preamble symbol will have M orthogonal bands, where a band is a group of contiguous subcarriers. Each tower is expected to transmit a preamble sequence in the band allocated to it. A modified version of the Schmidl-Cox method [16] can be used for CFO estimation, where the phase between the same band of adjacent preamble symbols is used to calculate the CFO of a signal from a particular tower. A hypothesis test to detect the presence or absence of a preamble sequence in each band will yield the number of interferers present.

in our model, the Doppler contribution is assumed to be less than 10%³ of the total CFO error. Since the oscillators in the towers are typically of high accuracy and the oscillators in the UE have lower accuracy, the VCO contribution can all be assumed to be in the same direction, i.e., all the CFO terms will have the same sign.

- 6) The base station equipment on all towers are assumed to use approximately the same sampling rate and subcarrier bandwidth.

The JmLS framework implicitly exploits the sparse nature of the multipath channel impulse response. Let the maximum multipath delay spread among all the channels be denoted by L and the number of towers present in a region in total be M . Then if $LM < N_p$, the number of pilots, the JmLS framework can be used. The JmLS gives the channel estimates of the desired as well as interference channels required to define the joint LLR detector. It is also an efficient scheme in the sense that the estimation performance improves as the number of significant interferers reduces. This is not possible in traditional orthogonal pilot tone based mLS, where the pilot allocation is fixed. Thus, the combination of JmLS and Joint LLR along with coded OFDM provides for a CFO-tolerant solution for the ITI scenario considered in the measurement model.

III. CARRIER FREQUENCY OFFSET COMPENSATION

In this section, a mathematical model is developed for the system based on the interference-free system model described in [15]. When all UEs have different CFOs, it is observed that the individual constellations of the different transmitters are rotated by an amount corresponding to the respective offset after down-conversion at the receiver. The time domain expression for the n^{th} sample of the i^{th} received OFDM symbol (after CP removal) is :

$$y_i(n) = e^{j2\pi \frac{(i(N+N_{cp})+N_{cp}+n)\epsilon_0}{N}} s_{i,0}(n) + e^{j2\pi \frac{(i(N+N_{cp})+N_{cp}+n)\epsilon_1}{N}} s_{i,1}(n) + \dots + e^{j2\pi \frac{(i(N+N_{cp})+N_{cp}+n)\epsilon_{M-1}}{N}} s_{i,M-1}(n) + w_i(n) \quad (1)$$

where s_m is the convolution of x_m and h_m , and denotes the faded OFDM symbol from the m^{th} tower. Here x_m is the transmit symbol and h_m is the Channel Impulse Response (CIR). The last term $w_i(n)$

³As an example, consider a UE with 1 ppm error and base stations with 0.1 ppm error. Then, the total CFO error 1.1 ppm corresponds to ± 550 Hz for a 500 MHz carrier frequency. Even if we consider user mobility of, say, 90 kmph (25 m/s), it translates to ± 42 Hz Doppler, which is below 10% of the CFO error. Since the VCO error is the primary contributor to CFO, the effect of Doppler can be neglected, and all CFO errors can be assumed to be in the same direction at the UE baseband.

is an AWGN noise sample. The frequency domain measurements for the k^{th} subcarrier can now be written as follows, where the symbol index i has been omitted for notational convenience:

$$Y[k] = e^{j2\pi \frac{(i(N+N_{cp})+N_{cp})\epsilon_0}{N}} \times e^{j\pi\epsilon_0 \frac{N-1}{N}} \frac{\sin(\pi\epsilon_0)}{N \sin\left(\frac{\pi\epsilon_0}{N}\right)} H_{k,0} X_0[k] + \sum_{m=1}^{M-1} e^{j2\pi \frac{(i(N+N_{cp})+N_{cp})\epsilon_m}{N}} \times e^{j\pi\epsilon_m \frac{N-1}{N}} \frac{\sin(\pi\epsilon_m)}{N \sin\left(\frac{\pi\epsilon_m}{N}\right)} H_{k,m} X_m[k] + ICI + W[k] \quad (2)$$

where $H_{k,m}$ is the Channel Frequency Response (CFR) and $X_m[k]$ is the symbol placed in the k^{th} subcarrier for the m^{th} tower. The term ICI in (2) is the inter subcarrier interference caused by the carrier frequency offset, and the measurement noise is zero mean and Gaussian with $W[k] \sim \mathcal{N}(0, \sigma^2)$. Now, the terms independent of the OFDM symbol index i in the above expression can be modelled by a modified frequency response H' :

$$Y[k] = e^{j2\pi \frac{(i(N+N_{cp}))\epsilon_0}{N}} \times H'_{k,0} X_0[k] + \sum_{m=1}^{M-1} e^{j2\pi \frac{(i(N+N_{cp}))\epsilon_m}{N}} \times H'_{k,m} X_m[k] + ICI + W[k] \quad (3)$$

where H' is an amplitude attenuated and phase rotated version of H . Using the pilot subcarriers, H' can be estimated in every p^{th} symbol. In our work, the channel is estimated in the first symbol and data is transmitted over the next $p - 1$ symbols before the channel is estimated again. Then, i will be given the index values $0, 1, 2, \dots, p - 1$, and again it wraps back to 0. According to (3), in addition to channel estimates, there is an additional normalized offset ϵ_m -dependent ‘‘phase ramping’’ which will cause a progressive phase shift for the data symbols received. This extra phase factor should be known while deriving the joint detector. For this, knowledge of CFOs ϵ_m are required. Defining the phase ramp term as $C_m = e^{j2\pi \frac{(i(N+N_{cp}))\epsilon_m}{N}}$, we can rewrite (3) as

$$Y[k] = C_0 H'_{k,0} X_0[k] + \sum_{m=1}^{M-1} C_m H'_{k,m} X_m[k] + \sum_{m \in \mathcal{M}} C_m I_{l,k}(m) + W[k] \quad (4)$$

where $I_{l,k}(m)$ is the ICI term between subcarriers l and k from the m^{th} tower. This can be explicitly

expanded as

$$I_{l,k}(m) = e^{j2\pi\frac{N_{cp}}{N}\epsilon_m} \sum_{l=0, l \neq k}^{N-1} \frac{\sin(\pi(l-k+\epsilon_m))}{N\sin(\pi(l-k+\epsilon_m)/N)} H_{k,m} X_m[k] e^{j\pi(l-k+\epsilon_m)\frac{N-1}{N}} \quad (5)$$

where $I_{l,k}(m) = 0$ when $\epsilon_m = 0$, and it increases with increasing values of ϵ_m . If interference is not present, the traditional time domain phase derotator [19] could be used to limit the CFO induced ICI. Since the user has access only to the received signal $y_i(n)$, each interference term cannot be individually de-rotated. Thus, an optimal de-rotation factor for the time domain signal needs to be determined.

In the presence of interference, each term $I_{l,k}(m)$ contributes to ICI. Derotation causes the ϵ_m in $I_{l,k}(m)$ to be replaced by $(\epsilon_m - \epsilon_*)$. It is seen from (5) that the ICI increases with increasing ϵ_m . The de-rotation factor to minimize the ICI can be found by solving for an ϵ_* that minimizes $|\epsilon_m - \epsilon_*|$ for all m . This is equivalent to minimizing the sum squared error of normalized offsets. That is,

$$\min_{\epsilon_*} \left(\sum_{m \in \mathcal{M}} \epsilon_m - M\epsilon_* \right)^2 \quad (6)$$

The solution to the above problem is then

$$\epsilon_* = \frac{1}{M} \sum_{m \in \mathcal{M}} \epsilon_m = \bar{\epsilon} \quad (7)$$

Thus, the received symbol is multiplied by $e^{-j2\pi\bar{\epsilon}\frac{n}{N}}$ before the CP removal. We call this method of de-rotation as ‘‘mean derotation’’ or ‘‘mean-centering’’ of the received constellation, as it distributes the new frequency offsets around zero offset almost uniformly. This operation causes all ϵ_m inside H' to be replaced by $\tilde{\epsilon}_m = \epsilon_m - \bar{\epsilon}$ in the frequency domain expressions. The ICI term also gets modified with all the ϵ_m in (5) inside the summation becomes $\tilde{\epsilon}_m$. This residual ICI is denoted by $\tilde{I}_{l,k}(m)$. Thus, (2) becomes,

$$Y_D[k] = C_0 e^{j2\pi N_{cp} \frac{\tilde{\epsilon}_0}{N}} \times e^{j\pi\tilde{\epsilon}_0 \frac{N-1}{N}} \frac{\sin(\pi\tilde{\epsilon}_0)}{N\sin\left(\frac{\pi\tilde{\epsilon}_0}{N}\right)} H_{k,0} X_0[k] + \sum_{m=1}^{M-1} C_m e^{j2\pi N_{cp} \frac{\tilde{\epsilon}_m}{N}} \times e^{j\pi\tilde{\epsilon}_m \frac{N-1}{N}} \frac{\sin(\pi\tilde{\epsilon}_m)}{N\sin\left(\frac{\pi\tilde{\epsilon}_m}{N}\right)} H_{k,m} X_m[k] + \sum_{m \in \mathcal{M}} C_m \tilde{I}_{l,k}(m) + W_1[k] \quad (8)$$

i.e.,

$$Y_D[k] = C_0 \tilde{H}_{k,0} X_0[k] + \sum_{m=1}^{M-1} C_m \tilde{H}_{k,m} X_m[k] + \sum_{m \in \mathcal{M}} C_m \tilde{I}_{l,k}(m) + W_1[k] \quad (9)$$

Here, the subscript “ D ” denotes time domain phase derotation, and we will call this equation as the *detection form*, since the joint detector would be derived from this. In vector form, (9) is given by:

$$\mathbf{Y}_D = C_0 \mathbf{X}_0 \mathbf{F}_L \tilde{\mathbf{h}}_0 + C_1 \mathbf{X}_1 \mathbf{F}_L \tilde{\mathbf{h}}_1 + \dots + C_{M-1} \mathbf{X}_{M-1} \mathbf{F}_L \tilde{\mathbf{h}}_{M-1} + \mathbf{W}' \quad (10)$$

During estimation, the value of index i is reset to 0 making all constants $C_m = 1$. This vectorized model is then called the *estimation form*, since it would be used to derive the joint channel estimator. Here, \mathbf{X}_m is a matrix with the pilot symbols along the diagonal, \mathbf{F}_L is a *sampled* version of DFT matrix of size N , with the rows corresponding to the pilot positions and the first L columns selected. The overall multipath delay spread T_m is measured from the signal and all significant ITI terms, and multiplied with the sampling frequency F_s to obtain L . If the overall delay is not known, $L = N_{cp}$ is assigned. The vectors $\tilde{\mathbf{h}}_m$ are $L \times 1$ vectors with elements corresponding to the first L taps of the CIR from the m^{th} base station to the UE, with the effects of residual offset also factored in. Finally, in (10), \mathbf{W}' is the combined residual ICI plus noise term. This model is an extension of the model proposed in [8] for the case of co-channel interferers.

IV. JOINT MODIFIED LEAST SQUARES

A. Channel Estimator

The Joint modified Least Squares Estimator, which has been compensated for frequency offset using *Mean Derotation*, will now be derived. Rewriting (10) as

$$\mathbf{Y}_D = \begin{bmatrix} \mathbf{X}_0 & \mathbf{X}_1 & \dots & \mathbf{X}_{M-1} \end{bmatrix} \begin{bmatrix} \mathbf{F}_L & \mathbf{0} & \dots & \mathbf{0} \\ \mathbf{0} & \mathbf{F}_L & \dots & \mathbf{0} \\ \dots & \dots & \dots & \dots \\ \mathbf{0} & \mathbf{0} & \dots & \mathbf{F}_L \end{bmatrix} \begin{bmatrix} \tilde{\mathbf{h}}_0 \\ \tilde{\mathbf{h}}_1 \\ \dots \\ \tilde{\mathbf{h}}_{M-1} \end{bmatrix} + \mathbf{W}' \quad (11)$$

i.e.,

$$\mathbf{Y}_D = \mathbf{X} \mathbf{F}_{LM} \tilde{\mathbf{h}}_{LM} + \mathbf{W}'. \quad (12)$$

where \mathbf{X} represents the concatenated matrix $[\mathbf{X}_0 \ \mathbf{X}_1 \ \dots \ \mathbf{X}_{M-1}]$, $\underline{\mathbf{F}}_{LM}$ represents the block diagonal matrix with \mathbf{F}_L as the block diagonal elements, and $\tilde{\mathbf{h}}_{LM}$ is an $LM \times 1$ vector with M subvectors $\tilde{\mathbf{h}}_i$ of size $L \times 1$. This can be solved for an estimate of $\hat{\mathbf{h}}_{LM}$ by the following optimization:

$$\min_{\tilde{\mathbf{h}}_{LM}} \|\mathbf{W}'\|^2 = \min_{\tilde{\mathbf{h}}_{LM}} \|\mathbf{Y}_D - \mathbf{X}\underline{\mathbf{F}}_{LM} \tilde{\mathbf{h}}_{LM}\|^2. \quad (13)$$

The solution of the above problem will be called *Joint-mLS*, and it yields

$$\hat{\mathbf{h}}_{JmLS} = (\underline{\mathbf{F}}_{LM}^H \mathbf{X}^H \mathbf{X} \underline{\mathbf{F}}_{LM} + \alpha \mathbf{I})^{-1} \underline{\mathbf{F}}_{LM}^H \mathbf{X}^H \mathbf{Y}_D. \quad (14)$$

where a real number $\alpha > 0$ is an appropriately chosen Tikhonov regularization factor [20]. This α is required because \mathbf{F}_L is a row *and* column subsampled version of the DFT matrix. Row sub-sampling may cause the DFT matrix to lose its orthogonality among columns and could make the inverse ill-conditioned.

It should be noted that the estimator could be pre-calculated for as many symbols for which the value of L remains constant. Thus, for slowly fading channels, the matrix inversion need not be done each time the channel is estimated. For channels which fade faster, L could be set as N_{cp} to avoid having to recompute the estimator.

The individual CIR estimates of each channel are obtained from (14) by extracting out the M subvectors of size $L \times 1$. The m^{th} subvector can be extracted by selecting the elements from $Lm + 1$ to $Lm + L$. Here m varies from 0 to $M - 1$. Finally, the channel frequency response is determined as

$$\hat{\mathbf{H}}_m = \mathbf{F}_L \hat{\mathbf{h}}_m. \quad (15)$$

B. Cramer Rao Lower Bound (CRLB)

The Cramer-Rao Bound on the variance of the channel impulse response estimate gives a lower bound on the mean squared error expected from an unbiased estimator of that parameter. For the purpose of determining CRLB, it is assumed that the pilots used are orthogonal in the code domain and that they occupy all the subcarriers available in the OFDM system. The model under consideration for such an M -tower system is thus,

$$\mathbf{Y} = \mathbf{X}\underline{\mathbf{F}}_{LM} \underline{\mathbf{h}}_{LM} + \mathbf{W} \quad (16)$$

where $\mathbf{W} \sim \mathcal{N}(\mathbf{0}, \sigma^2 \mathbf{I})$. Now, the noise vector can be rewritten as:

$$\mathbf{W} = \mathbf{Y} - \mathbf{X}\underline{\mathbf{F}}_{LM} \underline{\mathbf{h}}_{LM} \quad (17)$$

Since \mathbf{W} is a Gaussian vector, the log likelihood function of \mathbf{W} is given by

$$\ln p(\mathbf{W}, \underline{\mathbf{h}}_{LM}) = -\frac{N}{2} \ln (2\pi\sigma^2) - \frac{(\mathbf{Y} - \mathbf{X}\underline{\mathbf{F}}_{LM} \underline{\mathbf{h}}_{LM})^H (\mathbf{Y} - \mathbf{X}\underline{\mathbf{F}}_{LM} \underline{\mathbf{h}}_{LM})}{2\sigma^2} \quad (18)$$

Differentiating once w.r.t $\underline{\mathbf{h}}_{LM}$,

$$\nabla_{\underline{\mathbf{h}}_{LM}} \ln p(\mathbf{W}, \underline{\mathbf{h}}_{LM}) = -\frac{(-2\mathbf{Y}^H \mathbf{X}\underline{\mathbf{F}}_{LM} + 2\underline{\mathbf{h}}_{LM}^H \underline{\mathbf{F}}_{LM}^H \mathbf{X}^H \mathbf{X}\underline{\mathbf{F}}_{LM})}{2\sigma^2} \quad (19)$$

Differentiating again, we obtain

$$\nabla_{\underline{\mathbf{h}}_{LM}}^2 \ln p(\mathbf{W}, \underline{\mathbf{h}}_{LM}) = -\frac{(\underline{\mathbf{F}}_{LM}^H \mathbf{X}^H \mathbf{X}\underline{\mathbf{F}}_{LM})}{\sigma^2} \quad (20)$$

The Fisher Information matrix [11] is given by

$$\mathcal{I}(\underline{\mathbf{h}}_{LM}) = -E \left[\nabla_{\underline{\mathbf{h}}_{LM}}^2 \ln p(\mathbf{W}, \underline{\mathbf{h}}_{LM}) \Big| \underline{\mathbf{h}}_{LM} \right] = \frac{(\underline{\mathbf{F}}_{LM}^H \mathbf{X}^H \mathbf{X}\underline{\mathbf{F}}_{LM})}{\sigma^2}. \quad (21)$$

For unit amplitude polyphase pilots (e.g., M-ary PSK), $\mathbf{X}^H \mathbf{X} = \mathbf{I}$. Since $\underline{\mathbf{F}}_{LM}$ consists of orthogonal columns, $\underline{\mathbf{F}}_{LM}^H \underline{\mathbf{F}}_{LM} = N\mathbf{I}_{LM}$, an $LM \times LM$ identity matrix. Thus $\mathcal{I}(\underline{\mathbf{h}}_{LM}) = \frac{N}{\sigma^2} \mathbf{I}_{LM}$. The lower bound on the total variance of an estimate of $\underline{\mathbf{h}}_{LM}$ is given by $\text{trace}(\mathcal{I}^{-1}(\underline{\mathbf{h}}_{LM})) = \frac{M \times L}{N} \times \sigma^2$. In general, if pseudo-orthogonal pilots are used, CRLB is found as:

$$CRLB(\hat{\mathbf{h}}) = \text{trace} \left((\underline{\mathbf{F}}_{LM}^H \mathbf{X}^H \mathbf{X}\underline{\mathbf{F}}_{LM})^{-1} \right) \sigma^2 \quad (22)$$

In a similar manner, it can be shown that for orthogonal estimation using mLS, when the channel from the m^{th} tower to user is estimated by dividing the available pilots to M sets with N_p/M pilots each, the CRLB is given by:

$$CRLB(\hat{\mathbf{h}}_o) = \text{trace} \left((\mathbf{F}_{L1}^H \mathbf{X}_1^H \mathbf{X}_1 \mathbf{F}_{L1})^{-1} \right) \sigma^2 \quad (23)$$

where \mathbf{F}_{L1} is the sampled version of \mathbf{F}_L where only the rows corresponding to one of the subsets of pilots used for orthogonal subcarrier based estimation are selected. Thus, it will have N_p/M rows

rather than N_p rows. Also, \mathbf{X}_1 is the matrix with these N_p/M orthogonal pilots along its diagonal. If the matrix to be inverted is ill-conditioned, it would be regularized with an appropriate regularization factor.

A lower bound on the variance of the estimate of CIR can be found by imposing the orthogonal pilot assumption and assuming $(\mathbf{X}_1^H \mathbf{X}_1) = \mathbf{I}$. This is valid in the case of equal amplitude pilots (e.g., PSK pilots). Then, only $trace((\mathbf{F}_{L1}^H \mathbf{F}_{L1})^{-1})$ needs to be found. Now, $\lambda_i(\cdot)$ is defined as the function that gives the i^{th} eigenvalue of its argument. Since the trace is equal to the sum of eigenvalues and $\lambda_i((\mathbf{F}_{L1}^H \mathbf{F}_{L1})^{-1}) = (\lambda_i(\mathbf{F}_{L1}^H \mathbf{F}_{L1}))^{-1}$ for each individual eigenvalue λ_i , $trace((\mathbf{F}_{L1}^H \mathbf{F}_{L1})^{-1}) = \sum_{i=1}^L \lambda_i^{-1}$. The eigenvalues of $(\mathbf{F}_{L1}^H \mathbf{F}_{L1})$ will now be determined.

Assume that the pilot patterns for the different ITI signals are placed in different sets of orthogonal subcarriers that are uniformly distributed. For example, in a two tower system, tower 1 pilots can be placed in the odd subcarriers and tower 2 pilots can be placed in the even subcarriers. Thus, for M towers, N_p/M pilots are dedicated to estimate each tower to user channel. Then, \mathbf{F}_{L1} is obtained by subsampling \mathbf{F}_L by selecting the rows $\{1, M+1, 2M+1, \dots\}$. Practically, this matrix can be approximated by a lower order DFT matrix $\mathbf{F}^{(r)}$ of size N_p/M . It is found that the eigenvalues of $\mathbf{F}_L^{(r)H} \mathbf{F}_L^{(r)}$, where $\mathbf{F}_L^{(r)}$ consists of the first L columns of $\mathbf{F}^{(r)}$, is approximately equal to the eigenvalues of $\mathbf{F}_{L1}^H \mathbf{F}_{L1}$. The eigenvalue set of $\mathbf{F}^{(r)H} \mathbf{F}^{(r)}$ is N_p/M , repeated N times, and the eigenvalue set of $\mathbf{F}_L^{(r)H} \mathbf{F}_L^{(r)}$ is N_p/M , repeated L times. Thus, $trace((\mathbf{F}_{L1}^H \mathbf{F}_{L1})^{-1}) \approx \sum_{i=1}^L (N_p/M)^{-1} = \frac{L \times M}{N_p}$ and the CRLB will be approximately equal to $\frac{L \times M}{N_p} \sigma^2$. When pilots occupy all available subcarriers, $N_p = \lfloor \frac{N}{M} \rfloor M \approx N$. Then, the $CRLB(\hat{\mathbf{h}}_o) \approx \frac{L \times M}{N} \sigma^2$. This is for one channel. For the M uncorrelated channels, the CRLB add together and the total lower bound on variance is $\approx \frac{L \times M^2}{N} \sigma^2$. Comparing with the CRLB for JmLS for M interferers, which was found earlier to be $\frac{L \times M}{N} \sigma^2$ for orthogonal pilots used in all N subcarriers, the reduction in estimate variance when using the Joint-mLS algorithm is a factor of M , or $10 \log_{10} M$ dB.

It should be noted that this gain is due to the increased number of pilots available in JmLS due to the non-orthogonal nature of pilot subcarriers. However, this gain can be nullified if the orthogonal subcarrier allocation based mLS system sends pilots with boosted power. This is possible because in such an orthogonal scheme, all other towers have null subcarriers in those frequency locations where a specific tower sends pilot subcarriers to estimate the channel. Thus, the pilot power in orthogonal systems can be boosted by a factor of M while keeping the same power per symbol as JmLS.

It is worth mentioning here that the advantage of JmLS would become evident if $N_p/4$ pilots are used instead of N_p and the freed up subcarriers are used to improve either the code rate of the data transmission or the data rate. The former case will be illustrated in the simulation results section.

C. CRLB achieving estimator

Calculation of the mean squared error of the JmLS estimate reveals that this estimator achieves CRLB. The JmLS estimator for (16) is given by equating (19) to zero and solving for $\underline{\mathbf{h}}_{LM}$, which was found to be

$$\hat{\underline{\mathbf{h}}}_{LM} = (\underline{\mathbf{F}}_{LM}^H \mathbf{X}^H \mathbf{X} \underline{\mathbf{F}}_{LM})^{-1} \underline{\mathbf{F}}_{LM}^H \mathbf{X}^H \mathbf{Y} \quad (24)$$

Substituting (16) in the above, the estimation error vector is found to be

$$\mathcal{E} = (\underline{\mathbf{F}}_{LM}^H \mathbf{X}^H \mathbf{X} \underline{\mathbf{F}}_{LM})^{-1} \underline{\mathbf{F}}_{LM}^H \mathbf{X}^H \mathbf{W} \quad (25)$$

where \mathbf{W} is a zero-mean additive white Gaussian noise which is subjected to a sequence of matrix operations. Since all matrix multiplications are linear transformations [21], the linear transformation of a jointly Gaussian random vector is also Gaussian [22]. The estimation operation does not change the mean or distribution of the noise, and since the estimation error is zero-mean, the estimator proposed is *unbiased*. For unbiased estimates, the mean squared error of the estimate will be equal to its variance. The estimator is said to achieve CRLB if the MSE is found to be equal to the CRLB computed in the previous section.

$$MSE = trace(\mathcal{E}\mathcal{E}^H) = trace\left(\frac{\sigma^2}{N} \mathbf{I}_{LM}\right) = \frac{M \times L}{N} \times \sigma^2 \quad (26)$$

Here, it is assumed that all the subcarriers of an OFDM symbol are used for pilots, and that the pilots of different ITI terms are orthogonal to each other. The JmLS estimator achieves CRLB under the given assumptions and is the MVUE for the channel estimation problem under consideration. These assumptions are required to obtain the simplified expression for the CRLB and MSE. When pilots are present only in a subset of subcarriers, regularization affects both the CRLB and the MSE values and it becomes difficult to obtain a closed form expression. Pseudo-orthogonality of pilots rather than true orthogonality leads to “cross-term” submatrices in the $\mathbf{X}^H \mathbf{X}$ matrix, which contributes to some

interference. However, simulations confirm that the amount of such interference leakage is small, and that the MSE decays linearly with SNR even if the assumptions of orthogonality and full band pilots do not hold. It will be seen that the residual ICI due to carrier frequency offset will cause flooring of MSE in high SNRs and is the primary reason for performance limitation of the JmLS. However, the channel estimation quality is found to be adequate, and this performance bottleneck is of very little practical consequence.

V. OFFSET CORRECTED JOINT LLR

A maximum likelihood detector for the problem considered can be found by referring back to the detection form (9). The Max-Log-MAP approach is used to determine bit-level LLR estimates for the desired data and pass these values to a soft decoder. As the message symbol originating from the 0^{th} tower is of interest, the LLR test of each bit in that symbol being a zero or a one is calculated while considering all the possibilities of transmitted symbols for the remaining towers. Other parameters like CFOs of each ITI signal (equivalently $C_m, m = 0, 1, \dots, M - 1$), the CFR from each tower, assumed knowledge of the signal constellations employed on the ITI waveforms are needed to compute this LLR. Practically, the CFRs of other base stations are estimated using JmLS and the CFOs are estimated using some of the established methods. For example, a few tracking pilots may be placed in all OFDM symbols and phase shift in the OFDM pilots can be measured [23].

The Joint LLR problem can be formulated while including the effect of CFO as

$$LLR_{0,\lambda,k} = \ln \left(\frac{P(b_\lambda(X_0[k]) = 1 \mid Y_D[k], \mathbf{C}, \tilde{\mathbf{H}}_k)}{P(b_\lambda(X_0[k]) = 0 \mid Y_D[k], \mathbf{C}, \tilde{\mathbf{H}}_k)} \right). \quad (27)$$

where the notation $b_\lambda()$ denotes the λ^{th} bit. Assuming that the residual ICI does not distort the Gaussianity much, the probabilities in the numerator and denominator would follow the Gaussian distribution. Then, applying Bayes Theorem,

$$LLR_{0,\lambda,k} = \ln \left(\frac{P(Y_D[k] \mid b_\lambda(X_0[k]) = 1, \mathbf{C}, \tilde{\mathbf{H}}_k) P(b_\lambda(X_0[k]) = 1)}{P(Y_D[k] \mid b_\lambda(X_0[k]) = 0, \mathbf{C}, \tilde{\mathbf{H}}_k) P(b_\lambda(X_0[k]) = 0)} \right) \quad (28)$$

Assuming equal prior probabilities for constellation points (and summing over all possibilities for which $b_\lambda(X_0[k]) = 1$ in the numerator and $b_\lambda(X_0[k]) = 0$ in the denominator), the marginal distribution of

the above is found from the joint distribution as

$$LLR_{0,\lambda,k} = \ln \left(\frac{\sum_{X_0 \in \mathbf{X}_0^{(1,\lambda)}} \sum_{\substack{X_m \in \mathbf{X}_m, \\ m \neq 0}} P(Y_D[k] \mid \mathbf{C}, \tilde{\mathbf{H}}_k, \mathbf{X}[k])}{\sum_{X'_0 \in \mathbf{X}_0^{(0,\lambda)}} \sum_{\substack{X_m \in \mathbf{X}_m, \\ m \neq 0}} P(Y_D[k] \mid \mathbf{C}, \tilde{\mathbf{H}}_k, \mathbf{X}[k])} \right). \quad (29)$$

Here $\mathbf{X}_0^{(1,\lambda)}$ denotes the subset of the constellation of \mathbf{X}_0 for which the λ^{th} bit is 1, and $\mathbf{X}_0^{(0,\lambda)}$ denotes the subset of the constellation of \mathbf{X}_0 for which the λ^{th} bit is 0. Again, proceeding under the Gaussian assumption, the joint LLR equation becomes:

$$LLR_{0,\lambda,k} = \ln \left\{ \frac{\sum_{X_0 \in \mathbf{X}_0^{(1,\lambda)}} \sum_{\substack{X_m \in \mathbf{X}_m, \\ m \neq 0}} \exp \left(-\frac{1}{\sigma^2} \|Y_D[k] - C_0 \tilde{H}_{k,0} X_0[k] + \sum_{m=1}^{M-1} C_m \tilde{H}_{k,m} X_m[k]\|^2 \right)}{\sum_{X'_0 \in \mathbf{X}_0^{(0,\lambda)}} \sum_{\substack{X_m \in \mathbf{X}_m, \\ m \neq 0}} \exp \left(-\frac{1}{\sigma^2} \|Y_D[k] - C_0 \tilde{H}_{k,0} X'_0[k] + \sum_{m=1}^{M-1} C_m \tilde{H}_{k,m} X_m[k]\|^2 \right)} \right\} \quad (30)$$

The complexity of the detector is reduced by using the suboptimal Max-Log-MAP approximation proposed in [14]; i.e.,

$$LLR_{0,\lambda,k} \approx \min_{\substack{X_0 \in \mathbf{X}_0^{(1,\lambda)}, \\ X_m \in \mathbf{X}_m, m \neq 0}} \frac{1}{\sigma^2} \|Y_D[k] - C_0 \tilde{H}_{k,0} X_0[k] + \sum_{m=1}^{M-1} C_m \tilde{H}_{k,m} X_m[k]\|^2 \\ - \min_{\substack{X'_0 \in \mathbf{X}_0^{(0,\lambda)}, \\ X_m[k] \in \mathbf{X}_m, m \neq 0}} \frac{1}{\sigma^2} \|Y_D[k] - C_0 \tilde{H}_{k,0} X'_0[k] + \sum_{m=1}^{M-1} C_m \tilde{H}_{k,m} X_m[k]\|^2 \quad (31)$$

Thus, knowledge of the frequency offsets can help us modify the Joint LLR equation to incorporate the effect of CFO. Note, however, that the effect of residual ICI could still persist in the receiver, and it is considered to be a part of the ‘‘effective’’ noise in the above approximation. The LLR expression also includes the phase ramp term C_m which was seen in (9). This term tracks the phase change in the data symbols caused due to CFO. In the absence of this term in the JLLR expression, flooring due to CFO-induced ICI occurs. Equation (31) is called the Offset Corrected Joint LLR (OC-JLLR). For convenience, the prefix ‘‘Offset Corrected’’ is dropped hereafter when it is obvious from the context.

When no interferers and no CFO are present, this is the setup for the minimum distance receiver. When CFO and interferers are present, the M -tuple $(C_0 \tilde{H}_{k,0} X_0, C_1 \tilde{H}_{k,1} X_1, \dots, C_{M-1} \tilde{H}_{k,M-1} X_{M-1})$

represents the rotated super-constellation, whereas the M -tuple $(X_0, X_1, \dots, X_{M-1})$ is the super-constellation at the receiver in the absence of noise, fading and ICI. Thus, the distance of the received symbol from its ideal position at the receiver is measured here. The difference is usually non-zero and is caused by fading channel, noise and ICI in the system.

VI. SIMULATION RESULTS AND DISCUSSION

A system with up to 3 ITI signals is considered for simulations. A carrier frequency of 500 MHz and a sampling frequency of 30.72 MHz are assumed for the 20 MHz OFDM signal. For a subcarrier bandwidth of 15 kHz, this gives $N = 2048$ subcarriers. In each OFDM symbol, 1200 subcarriers are used for pilots or data and the remaining constitute the guard band and the DC subcarrier. In the initial simulations, a uniform power delay profile is used for the interferers to avoid any bias in the results due to the power distribution in the multipaths. Each non-zero CIR coefficient is chosen independently from a Rayleigh distribution. The path delays are assumed following the IEEE Pedestrian-A [24] channel model $([0, 110, 190, 410] \times 10^{-9} \text{ s})$. The three interferers are delayed by 450 ns, 650 ns and 1650 ns relative to the first multipath component of the desired signal having a (relative) delay of 0 ns. Here, the PDPs of interferers 1 and 2 have 50% overlap, but this does not affect the results in any way. The CFOs are randomly assigned between 0 and Δf_{max} in the beginning of each frame. Here, a frame consists of the first symbol used for estimation followed by six information bearing symbols. The effect of CFO compensation is evaluated by comparing the proposed mean offset derotation, derotation using the maximum offset Δf_{max} , and no derotation schemes. Turbo coding with a code rate of 1/3 is used for simulations.

A. Joint estimation of desired and ITI channels

The mean squared error (MSE) between the true value and the estimate is used to measure the quality of channel estimates. The MSE performance for the CIR as well as the CFR estimate is plotted against the SNR per bit (E_b/N_0).

In Fig. 2, the simulated total MSE of the JmLS CIR estimate, $\hat{\mathbf{h}}_{LM}$, is compared with the value predicted by the CRLB expression given by (22). QPSK symbols having low correlation are randomly generated to occupy all N subcarriers. The comparisons are performed for $M = 1, 2, 3, 4$ and for a benchmark comparison, estimation of the four channels using the conventional mLS proposed in [8] is

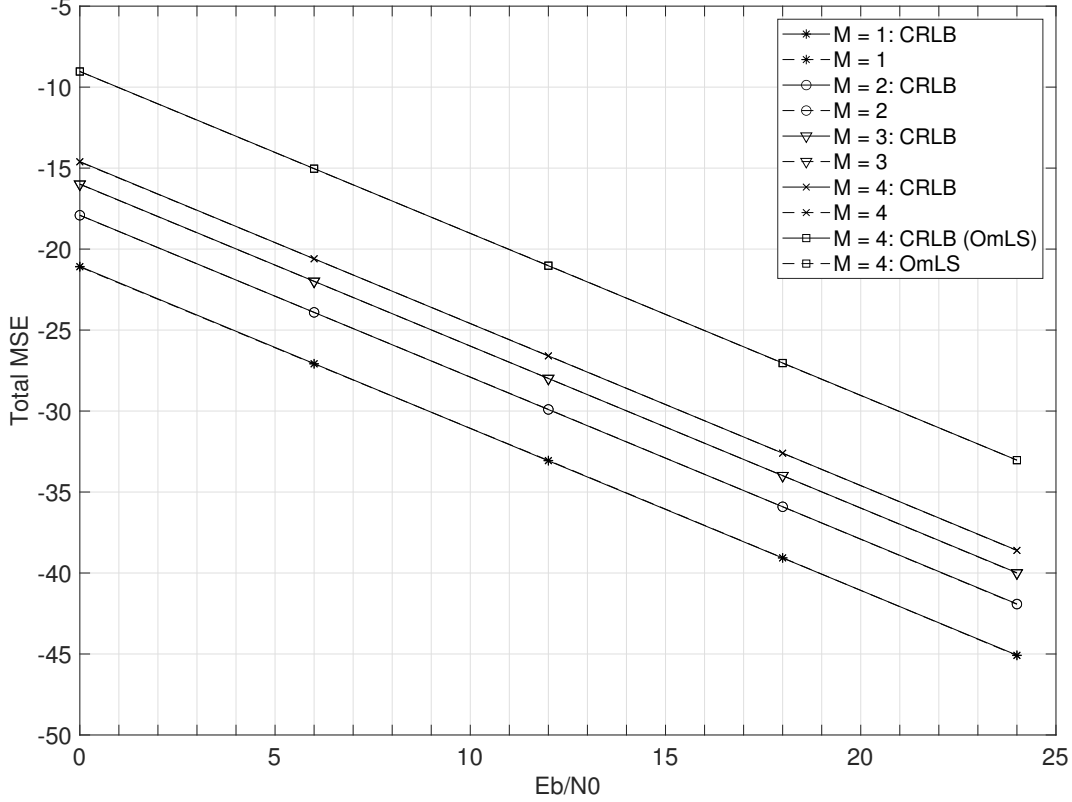


Fig. 2: Total MSE of JmLS estimate of CIR and the corresponding CRLB plotted for different number of interferers. CFO is not considered.

also included. For this purpose, N subcarriers are divided into four orthogonal sets having $N/4$ pilots each, and one pilot set is assigned to each tower. This estimate is called Orthogonal mLS (OmLS) to distinguish it from the proposed Joint mLS (JmLS) method, where pilots for different channels occupy the same set of N subcarriers. The four OmLS estimates are then concatenated and the total MSE is plotted in the figure for comparison. Next, the CRLB of the OmLS estimate is plotted.

The plot shows that the CIR estimate using orthogonal subcarriers is approximately 6dB worse when compared to the joint estimate for $M = 4$ case, which clearly shows the advantage of going for joint estimation. This result matches with the $10 \log_{10} M$ improvement predicted by the CRLB analysis shown earlier. It is seen that all the CRLB plots match with the MSE plots, showing that the estimator is MVUE.

It should be noted that this improvement in JmLS comes while assuming that the pilot power per subcarrier is the same for both JmLS and OmLS, and that JmLS uses all available subcarriers. The advantage of JmLS lies in the fact that since the pilots no longer need to be frequency orthogonal,

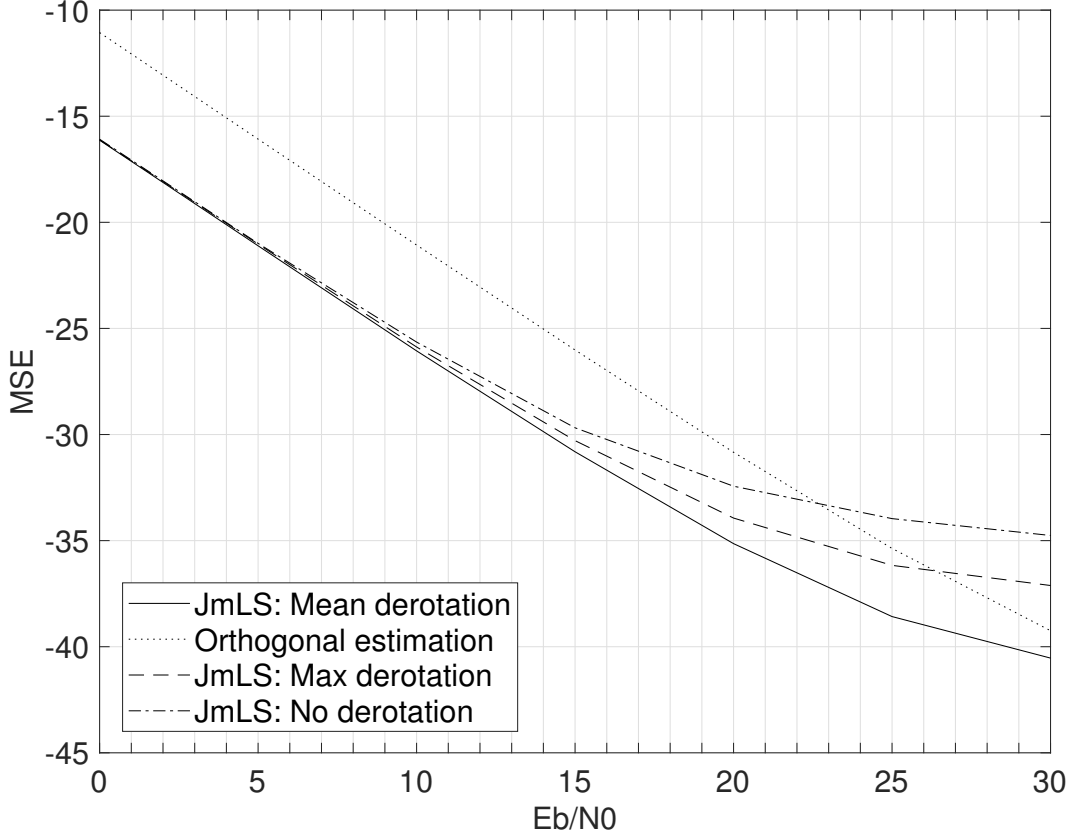


Fig. 3: MSE of CFR over the used subcarriers (1200 out of 2048) for OmLS versus JmLS with different offset derotations for $\Delta f_{max} = 750 \text{ Hz}$

M times the number of pilot subcarriers can be used when compared to OmLS. If the OmLS pilot is boosted by keeping the OFDM symbol power equal to that of JmLS, it is seen that the MSE performances become equal. Further, if JmLS is restricted to use N/M pilots like the OmLS scheme instead of N , JmLS will have a poorer performance. However, this arrangement frees $\frac{(M-1) \times N}{M}$ subcarriers for data transmission. These extra subcarriers could be used to provide a code rate improvement for high code rate systems by utilizing these vacant subcarriers as additional parity bits. Such a comparison brings out another advantage of joint estimation, and this will be investigated in a later section of this paper. Further advantages of JmLS will become obvious when it is combined with the Joint LLR method and the effect of frequency offset comes into play. Next, the performance of mean and maximum offset derotation techniques for offset compensation are considered. The simulation results in Fig. 3 shows the per subcarrier MSE of the CFR estimate for JmLS as well as OmLS plotted against E_b/N_0 . Approximately 6dB ($= 10 \log_{10}(4)$) improvement in joint estimation schemes is seen in the

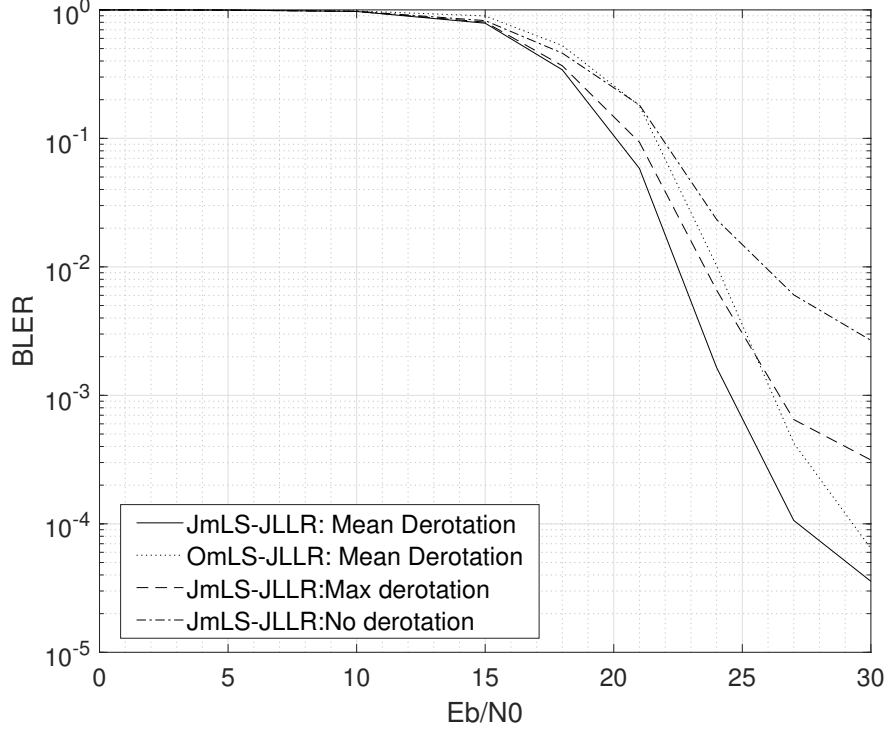


Fig. 4: Performance for different derotation techniques with 3 ITI signals, where all of them in power are 3 dB below the desired signal power.

CFR case as well. This improvement is a direct consequence of the improvement seen for the CIR estimates. At high SNRs, the effect of residual ICI manifests as flooring of the MSE curve. It is seen that JmLS with mean offset derotation is least affected by ICI induced flooring among all the joint estimation methods.

B. Joint detection using channel estimates

The Joint LLR approach proposed earlier is employed by the user to detect the data while accounting for the interference structure and noise statistics. The user equipment is required to estimate the channel distortion and the CFO induced distortion from all the (significant) co-channel signals in order to decode the message bits from the desired tower. The CFO distortion is implicitly captured by the JmLS channel estimates obtained. At the receiver, a frequency offset de-rotation is affected on the received time domain symbol. This is followed by the FFT operation. The derotated data \mathbf{Y}_D , a noise variance estimate, and the JmLS channel estimates are then fed to the Joint LLR computation block.

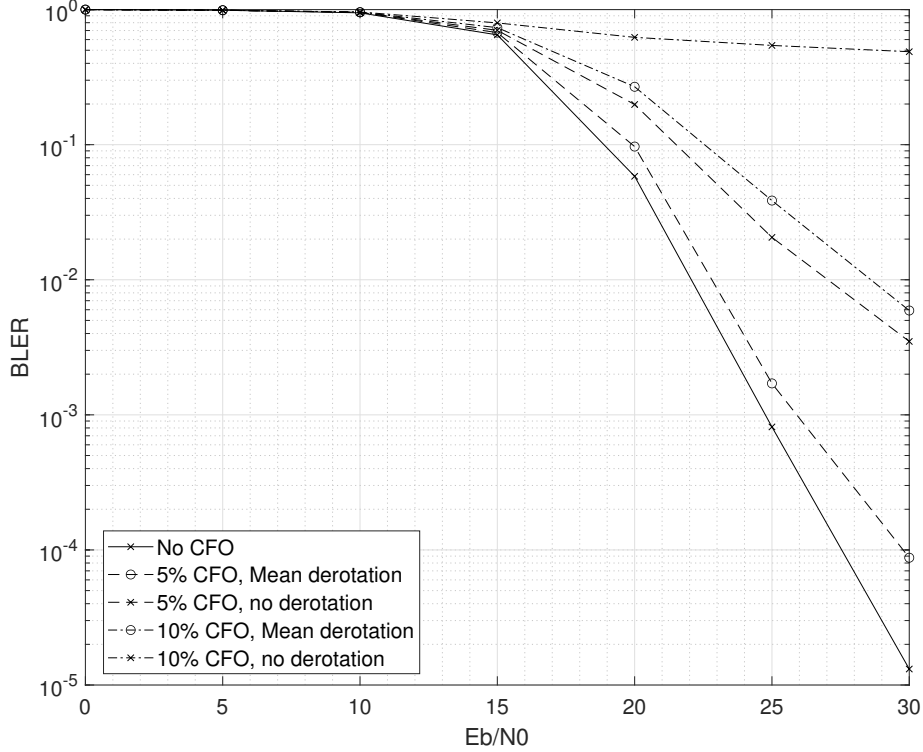


Fig. 5: Performance for different Δf_{max} as a percentage of subcarrier bandwidth.

Fig. 4 shows the effect of different time domain derotation techniques on the Block Error Rate (BLER) of a rate 1/3 Turbo coded OFDM system having a block length of 796. Here, a maximum carrier frequency offset of 750 Hz between the desired signal and the ITI signals is considered. JmLS-JLLR with mean offset derotation emerges as the better approach when compared to maximum offset derotation. In this particular scenario, it is seen that maximum offset derotation performs worse than having no derotation. After mean offset de-rotation, the residual offsets are distributed equally around zero and the mean residual offset becomes zero. This minimizes the ICI, as shown earlier.

The effect of Carrier Frequency Offset magnitude in the JmLS-JLLR framework is now studied to understand how much mean derotation improves the performance as compared to having no derotation. In Fig. 5, three different maximum CFO are considered: $\Delta f_{max} = 0$ Hz, 750 Hz and 1500 Hz, which corresponds to the cases of no CFO, CFO at 5% of subcarrier bandwidth and CFO at 10% of subcarrier bandwidth. It is seen that even if the CFO is 5% of subcarrier bandwidth, mean derotation brings the performance of the detector close to the case of having no CFO. Even at higher offsets, the derotation

continues to provide significant BLER performance gains.

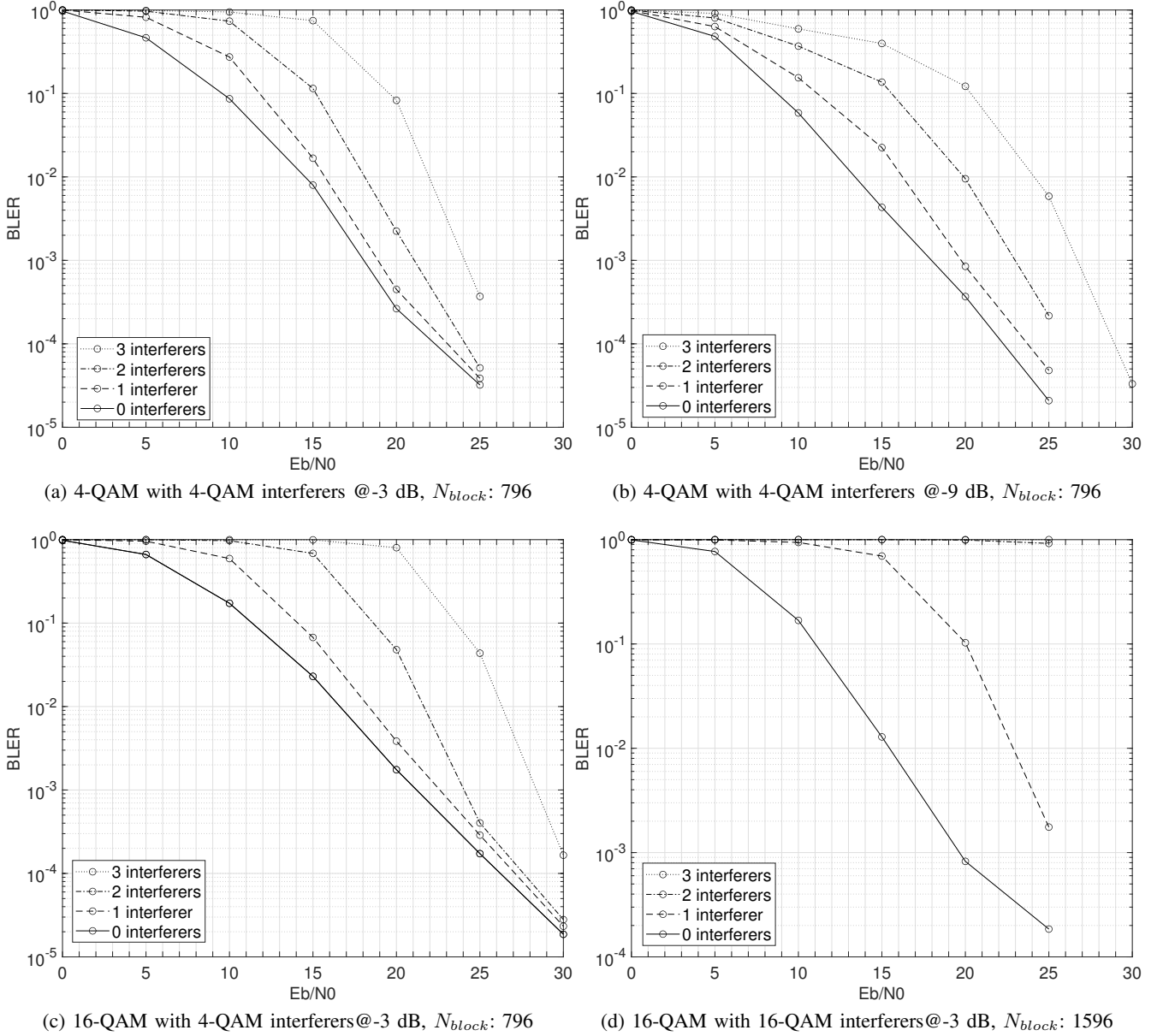


Fig. 6: BLER performance of JmLS-JLLR framework for 4-QAM and 16-QAM interferers. $\Delta f_{max} = 40Hz$.

Finally, the effect of adding interferers in the BLER performance is studied in the proposed framework. The performance of JmLS-JLLR is studied with interference scenarios $M = 2, 3$ and 4. The performance of ordinary mLS and ordinary LLR based detection in the absence of interferers is plotted as a benchmark for comparison. In Fig. 6a, this performance is plotted for 4-QAM message with additional 4-QAM interferers whose powers are 3 dB below it. Fig. 6b shows what happens when

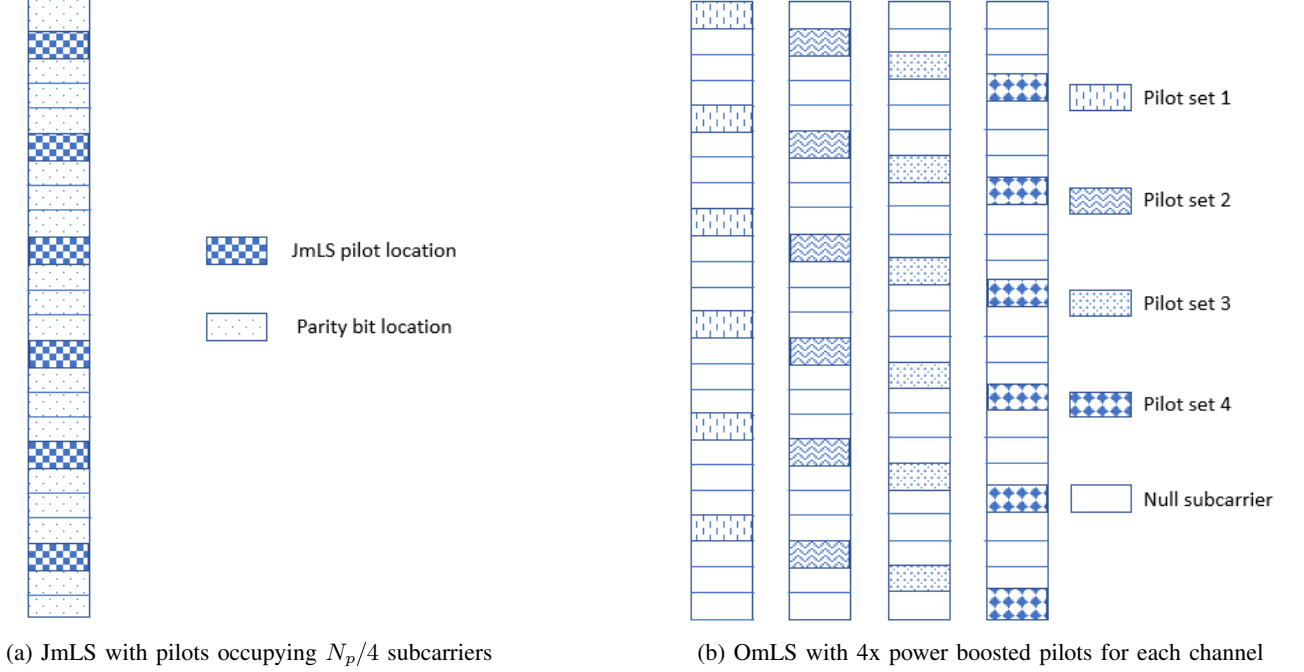


Fig. 7: Pilot allocation for (a) joint and (b) orthogonal schemes

the interferer powers are even lower. It is interesting to note that for lower interference powers, the performance actually degrades. This is expected since the quality of channel estimates of the interferers are adversely affected by their lower power. Thus, the effectiveness of accounting for interferer in Joint LLR decreases and performance degrades. At lower powers for the ITI terms, a more effective approach is to consider the interference as equivalent noise. Fig. 6c shows how a system with 16-QAM message and 4-QAM interferers behave and Fig. 6d shows what happens when interferers are also 16-QAM. Clearly, it shows that 4-QAM interferers are tolerated much better as compared to 16-QAM.

C. Code rate improvement

Next, the JmLS-JLLR framework performance in high code rate systems is investigated to see how it could bring about a rate improvement. This is made possible by utilizing the vacant subcarriers that would normally be reserved for OmLS based channel estimation. For this simulation, a power delay profile according to the IEEE Pedestrian-A channel model is considered. Here, the three interferers ($M=4$) have the same power as that of the message signal. JmLS-JLLR with a code rate of $3/4$ is compared with OmLS-JLLR with a code rate of $3/4$. It should be noted here that JmLS uses $N_p/4$ pilots, the same as OmLS. Further, OmLS boosts its pilot power by a factor of M because the subcarriers

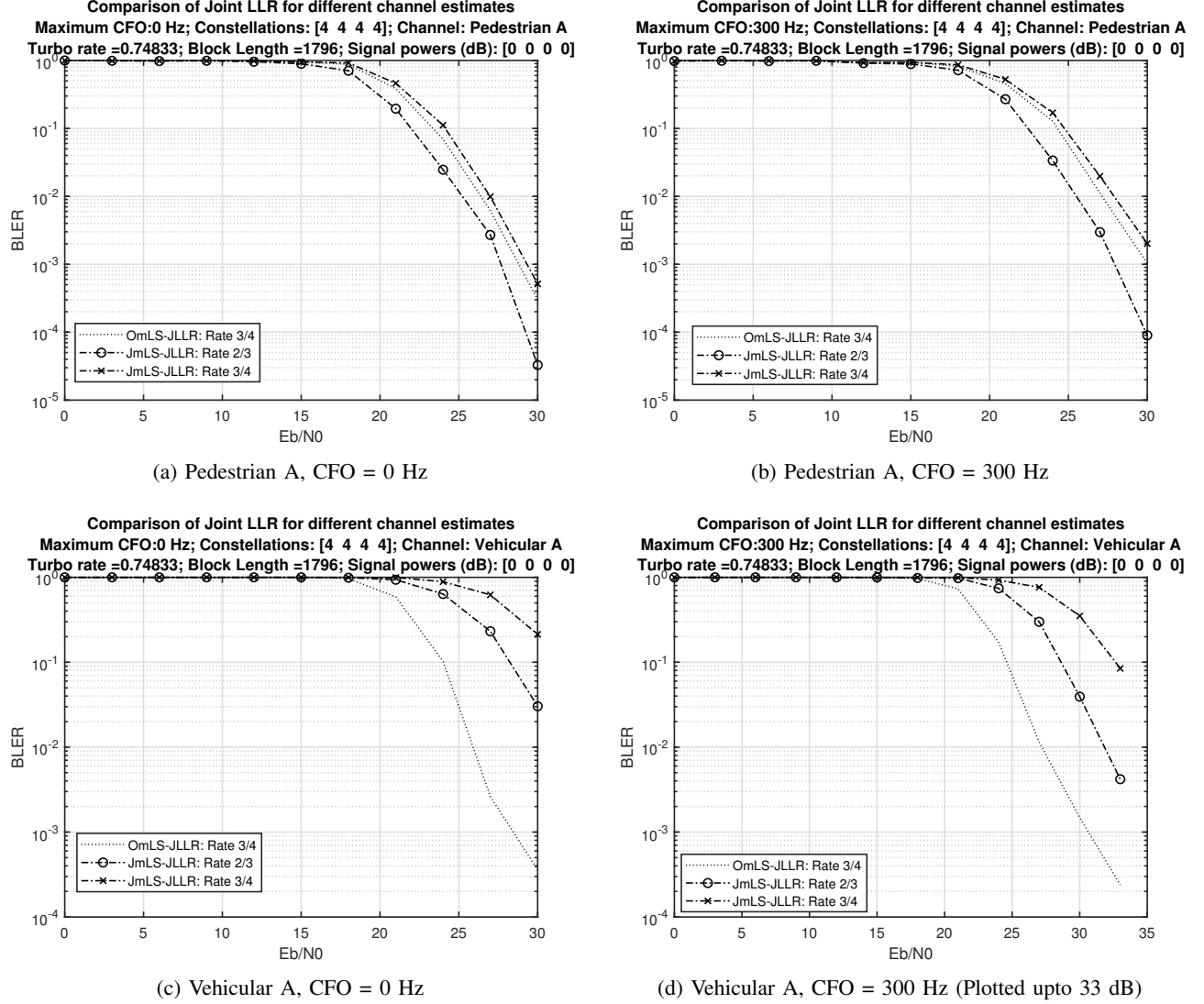


Fig. 8: BLER performance of Code Rate improvement scheme based on JmLS-JLLR framework for channels of low and high selectivity at different CFOs.

other than pilots are kept as null subcarriers. However, $\frac{(M-1) \times N}{M} = \frac{3N_p}{4}$ vacant subcarriers are now available for carrying data symbols and they will now be used for code rate improvement. The resulting pilot allocation is captured in Fig. 7.

In this specific simulation, the channel is estimated in every 7th OFDM symbol and coded data of rate 3/4 is sent in the remaining 6 OFDM symbols. When JmLS is employed, $\frac{3N_p}{4}$ subcarriers in the OFDM symbols $\{0, 7, 14, \dots\}$ could be used to fill additional parity bits of coded data from the remaining 6 OFDM symbols. Using this strategy, it is possible to obtain a code rate improvement from rate 3/4 to rate 2/3. If the vacant subcarriers in JmLS are not used for code rate improvement, then it is seen that

pilot power boosted OmLS performs better than JmLS. Due to this code rate improvement, it is seen that for channels with low selectivity (e.g., IEEE Pedestrian-A), Code Rate Improvement+JmLS-JLLR performs better than boosted pilot + OmLS-JLLR, which in turn performs better than JmLS-JLLR without any code rate improvement.

The simulation results are shown in Fig. 8. In the case of low selectivity as in IEEE Pedestrian-A channel model (Fig. 8a and 8b), it is found that the code rate improvement offered by using the vacant subcarriers due to JmLS formulation is sufficient to give an improved BLER performance as compared to the orthogonal framework. However, in the case of high selectivity as in IEEE Vehicular-A channel model (Fig. 8c and 8d), it is seen that the orthogonal estimation framework has lower BLER. This relative performance depends purely on the number of parity bits that could be incorporated in the vacant subcarriers of the estimation symbol. This code rate improvement brought about by the vacant subcarriers due to JmLS illustrates one of the possible advantages of joint estimation over orthogonal subcarrier based estimation.

VII. CONCLUSION

We have developed a joint channel estimation and detection framework for reuse-1 systems capable of mitigating the effect of interference by accounting for the interferers in the estimator and detector models. Even though the simulations were conducted for 500 MHz, similar performance gains are expected even at higher frequencies. The framework does not place any restrictions on the overlap of power delay profiles of the different channels, unlike prior works. It is best suited when the signal and interference are of comparable powers but will work well for any interference power profile since it is a joint detector.

The JmLS with mean offset derotation is shown to be superior to orthogonal subcarrier based estimation in terms of spectral efficiency or availability of more pilots, depending on which scheme is preferred. It meshes seamlessly to the Joint LLR framework, which needs the interferer channel estimates and information on the distortion caused due to Carrier Frequency Offset. The advantage of mean offset derotation was clearly highlighted, and the effect of the number and constellation of additional interferers were studied. Finally, the utility of JmLS for freeing pilot subcarriers for code rate improvement was presented, showcasing a 12.5% improvement in the rate at nearly the same SNR.

REFERENCES

- [1] M. C. Necker, "Towards frequency reuse 1 cellular FDM/TDM systems," in *Proceedings of the 9th ACM international symposium on Modeling analysis and simulation of wireless and mobile systems*, pp. 338–346, ACM, 2006.
- [2] M. Raghavendra, S. Bhashyam, and K. Giridhar, "Interference rejection for parametric channel estimation in reuse-1 cellular OFDM systems," *IEEE Transactions on Vehicular Technology*, vol. 58, no. 8, pp. 4342–4352, 2009.
- [3] R. Ghaffar and R. Knopp, "Interference Suppression Strategy for Cell-Edge Users in the Downlink," *IEEE Transactions on Wireless Communications*, vol. 11, no. 1, pp. 154–165, 2012.
- [4] T. D. Novlan, R. K. Ganti, A. Ghosh, and J. G. Andrews, "Analytical Evaluation of Fractional Frequency Reuse for OFDMA Cellular Networks," *IEEE Transactions on Wireless Communications*, vol. 10, no. 12, pp. 4294–4305, 2011.
- [5] S. Gupta, S. Kumar, R. Zhang, S. Kalyani, K. Giridhar, and L. Hanzo, "Resource Allocation for D2D Links in the FFR and SFR Aided Cellular Downlink," *IEEE Transactions on Communications*, vol. 64, no. 10, pp. 4434–4448, 2016.
- [6] P. H. Moose, "A technique for orthogonal frequency division multiplexing frequency offset correction," *IEEE Transactions on Communications*, vol. 42, no. 10, pp. 2908–2914, 1994.
- [7] V. Kotzsch, J. Holfeld, and G. Fettweis, "Joint detection and CFO compensation in asynchronous multi-user MIMO OFDM systems," in *VTC Spring 2009-IEEE 69th Vehicular Technology Conference*, pp. 1–5, IEEE, 2009.
- [8] J.-J. Van De Beek, O. Edfors, M. Sandell, S. K. Wilson, and P. O. Borjesson, "On channel estimation in OFDM systems," in *1995 IEEE 45th Vehicular Technology Conference. Countdown to the Wireless Twenty-First Century*, vol. 2, pp. 815–819, IEEE, 1995.
- [9] A. Jeremic, T. A. Thomas, and A. Nehorai, "OFDM channel estimation in the presence of interference," *IEEE Transactions on Signal Processing*, vol. 52, no. 12, pp. 3429–3439, 2004.
- [10] V.-D. Nguyen, M. Patzold, F. Maehara, H. Haas, and M.-V. Pham, "Channel estimation and interference cancellation for MIMO-OFDM systems," *IEICE Transactions on Communications*, vol. 90, no. 2, pp. 277–290, 2007.
- [11] S. M. Kay, *Fundamentals of Statistical Signal Processing: Estimation Theory*. Prentice Hall PTR, 1993.
- [12] Vishnu O. C., V. Kumar, M. Madhusoodanan, and K. Giridhar, "Joint Uplink LLR Computation, Quantization, and Combining for Load-Balanced Small Cells," in *2016 IEEE Global Communications Conference (GLOBECOM)*, pp. 1–6, IEEE, 2016.
- [13] J. Lee, D. Toumpakaris, and W. Yu, "Interference mitigation via joint detection," *IEEE Journal on Selected Areas in Communications*, vol. 29, no. 6, pp. 1172–1184, 2011.
- [14] P. Robertson, P. Hoeher, and E. Villebrun, "Optimal and sub-optimal maximum a posteriori algorithms suitable for turbo decoding," *European Transactions on Telecommunications*, vol. 8, no. 2, pp. 119–125, 1997.
- [15] Y. S. Cho, J. Kim, W. Y. Yang, and C. G. Kang, *MIMO-OFDM wireless communications with MATLAB*. John Wiley & Sons, 2010.
- [16] T. M. Schmidl and D. C. Cox, "Robust Frequency and Timing Synchronization for OFDM," vol. 45, no. 12, pp. 1613–1621, 1997.
- [17] A. Gomaa, L. M. Jalloul, M. M. Mansour, K. Gomadam, and D. Tujkovic, "Max-Log-MAP Optimal MU-MIMO Receiver for Joint Data Detection and Interferer Modulation Classification," *IEEE Communications Letters*, vol. 20, no. 7, pp. 1389–1392, 2016.
- [18] S. Desai and K. Giridhar, "Low Complexity Quasi-MLM Modulation Classification based Optimal Overloaded MU-MIMO Receiver," in *2020 IEEE 91st Vehicular Technology Conference (VTC2020-Spring)*, pp. 1–5, 2020.
- [19] T.-D. Chiueh and P.-Y. Tsai, *OFDM baseband receiver design for wireless communications*. John Wiley & Sons, 2008.
- [20] N. Galatsanos and A. Katsaggelos, "Cross-validation and other criteria for estimating the regularizing parameter," in *[Proceedings] ICASSP 91: 1991 International Conference on Acoustics, Speech, and Signal Processing*, pp. 3021–3024 vol.4, 1991.

- [21] G. Strang, "Linear Algebra and Its Applications.," 2004.
- [22] R. G. Gallager, *Stochastic processes: theory for applications*. Cambridge University Press, 2013.
- [23] G. L. Stuber, J. R. Barry, S. W. Mclaughlin, Y. Li, M. A. Ingram, and T. G. Pratt, "Broadband MIMO-OFDM wireless communications," *Proceedings of the IEEE*, vol. 92, no. 2, pp. 271–294, 2004.
- [24] S. Ahmadi, R. Srinivasan, H. Choi, J. Park, J. Cho, and D. Park, "Channel models for ieee 802.16 m evaluation methodology document," *IEEE C802*, vol. 16, 2007.